Naval Research Laboratory

Washington, DC 20375-5000

AD-A220 421

The Effects of Wiggler Errors on Free Electron Laser Performance

E. ESAREY, W. MARABLE* AND C. M. TANG

Beam Physics Branch
Plasma Physics Division

University of Maryland, College Park, MD 20742

April 2, 1990

DTIC
ELECTE
APR 12 1990
S
B
D

90 04 12

REPORT DOCUMENTATION PAGE

1. AGENCY USE ONLY (Leave blank)	2. REPORT DATE	3. REPORT TYPE AND DATES COVERED
	1990 April 2	Interim

4. TITLE AND SUBTITLE

The Effects of Wiggler Errors on Free Electron Laser Performance

5. FUNDING NUMBERS

6. AUTHOR(S)

Esarey, E., Marable*, W., and Tang, C. M.

7. PERFORMING ORGANIZATION NAME(S) AND ADDRESS(ES)

Naval Research Laboratory
Washington, DC 20375-5000

8. PERFORMING ORGANIZATION REPORT NUMBER

PR-9M0214

9. SPONSORING/MONITORING AGENCY NAME(S) AND ADDRESS(ES)

ONR
Arlington, VA 22217

National Institute of Standards and Technology
Gaithersburg, MD 20899

10. SPONSORING/MONITORING AGENCY REPORT NUMBER

NRL Memorandum Report 6597

12a. DISTRIBUTION/AVAILABILITY STATEMENT

Approved for public release distribution; unlimited.

12b. DISTRIBUTION CODE

13. ABSTRACT (Maximum 200 words)

The effects of random wiggler magnetic field errors on free electron lasers is analyzed analytically and computationally. Wiggler field errors perturb the electron beam as it propagates and lead to a random walk of the beam centroid δx as well as cause deviations in the parallel beam energy $\delta\gamma_\parallel$ and in the relative phase of the electrons in the ponderomotive wave $\delta\psi$. The phase deviation $\delta\psi$ is identified as the single most important parameter characterizing the detrimental effects of wiggler errors. In order to avoid significant reduction in gain it is necessary for the phase deviation to be small compared to π. It is shown that transverse focusing of the electron beam is not effective in reducing the phase deviation (i.e., transverse focusing reduces the average phase deviation by 1/2). Furthermore, it is shown that the results of beam steering at the wiggler entrance reduces the average phase deviation at the end of the wiggler by 1/3. The detrimental effects of wiggler errors may be reduced by arranging the magent poles in an optimal ordering such that the magnitude of the phase deviation is minimized.

14. SUBJECT TERMS	15. NUMBER OF PAGES
Free electron lasers Random field errors	26
	16. PRICE CODE

17. SECURITY CLASSIFICATION OF REPORT	18. SECURITY CLASSIFICATION OF THIS PAGE	19. SECURITY CLASSIFICATION OF ABSTRACT	20. LIMITATION OF ABSTRACT
UNCLASSIFIED	UNCLASSIFIED	UNCLASSIFIED	SR

CONTENTS

DTIC
COPY
INSPECTE
4

THE EFFECTS OF WIGGLER ERRORS ON FREE ELECTRON LASER PERFORMANCE

1. Introduction

Intrinsic magnetic field errors δB are present in any realistic wiggler magnet. Such errors are unavoidable and arise from imperfections in the fabrication and assembly of wiggler magnets. State–of–the–art wiggler construction techniques yield rms field errors on the order[1] $(\delta B/B_w)_{rms} \simeq 0.1 - 0.5\%$. These field errors perturb the electron beam as it propagates through the wiggler and lead to i) a random walk of the beam centroid,[2-4] δx, ii) variations in the parallel beam energy,[5-8] $\delta\gamma_{\parallel}$, and iii) variations in the relative phase of the electrons in the ponderomotive potential,[5-8] $\delta\psi$. If left uncorrected, field errors ultimately decrease free electron laser (FEL) gain[2-8] (this reduction becomes more significant for long wigglers). Reduction in gain may occur from a loss of optical guiding (due to large δx) or from a loss of FEL resonance (due to large $\delta\psi$).

Past research, for the most part, has been primarily concerned with the random walk δx. It has been shown that the random walk δx may be effectively controlled by i) transverse beam focusing[3-8] (finite k_β, where k_β is the betatron wavenumber) and by ii) periodic beam steering.[2-8] By using either one or a combination of beam focusing and periodic steering, in principle, the random walk δx may be kept as small as desired. The major conclusions of the present work are the following. Given that the random walk δx may be effectively controlled, the phase deviation $\delta\psi$ may be identified as the single most important parameter characterizing the effects of wiggler errors.[5-8] In particular, in order to avoid significant reduction in gain, it is necessary that $|\delta\psi| < \pi$. In addition, transverse beam focusing is not effective in controlling $\delta\psi$. Specifically, it may be shown that at the wiggler end $\langle\delta\psi\rangle = (1/2)\langle\psi(k_\beta = 0)\rangle$, where $\langle\rangle$ signifies an ensemble average. Furthermore, beam steering may be used to reduce $|\delta\psi|$ when[8] $L_S < \lambda_\beta$, where L_S is the length over which the steering performed and $\lambda_\beta = 2\pi/k_\beta$. As an example, for $k_\beta = 0$ and one steering segment, $\langle\delta\psi\rangle = (1/3)\langle\delta\psi\rangle_N$, where $\langle\delta\psi\rangle_N$ is the value in the absence of steering.

As a further motivation, it is appropriate to consider some aspects of wiggler design. Typically, when "ordering" a wiggler from a vendor, limits are placed on δB_{rms} and $|\int dz\delta B|$. To meet these specifications, the vendor may arrange the magnet pole in an optimum sequence such that $|\int dz\delta B|$ is minimized. The present research indicates, however, that the optimum "figure of merit" to minimize is not the line integral $|\int dz\delta B|$, but the magnitude of the phase deviation $|\delta\psi|$.

2. Random Walk of the Beam Centroid

As the electron beam propagates through the wiggler, the electrons experience random velocity kicks $\delta v_\perp$ via the $v_\parallel \times \delta B_\perp$ random force. The equation of motion for the electron beam centroid motion including transverse gradients (weak focusing) is given by[6] $d^2\delta x/dz^2 = -k_\beta^2 \delta x + k_w a_w \delta \dot{B}_y/\gamma$, where k_w is the wiggler wavenumber, k_β is the betatron wavenumber ($k_\beta = k_w a_w/(\sqrt{2}\gamma)$ for a helical wiggler), $\delta\hat{B} = \delta B/B_w$, B_w is the ideal wiggler peak magnetic field, $a_w = eB_w/k_w mc^2$, γ is the relativistic factor of the electron beam and z is the axial propagation distance. This equation may be solved to give the random centroid motion[6]

$$\delta\beta_x = \frac{a_w k_w}{\gamma} \int_0^z dz' \cos k_\beta(z' - z)\delta\hat{B}_y(z') \tag{1a}$$

$$\delta x = -\frac{a_w k_w}{\gamma k_\beta} \int_0^z dz' \sin k_\beta(z' - z)\delta\hat{B}_y(z'), \tag{1b}$$

where $\delta\beta = \delta v/c$.

Given the precise functional dependence of the wiggler errors $\delta B(z)$ for a given wiggler, the above expressions may be used to calculate $\delta x(z)$ for that specific wiggler. However, one does not always know ahead of time the full functional dependence of $\delta B(z)$. Instead, one may know only certain statistical properties of the field errors, such as the rms value δB_{rms}. Hence, it is useful to consider an ensemble of statistically identical wigglers for which the statistical properties of the field errors are known. By performing appropriate averages over this ensemble, one may determine the mean $\langle Q \rangle$ and variance σ for a quantity Q and, hence, determine the most probable range of a single realization of Q. Throughout the following, $\delta B(z)$ is assumed[6] to be a random function with zero mean, finite variance and with an autocorrelation distance given by $z_{ac} \simeq \lambda_w/2$. Also, in the following, a helical wiggler will be assumed and generalization of the results for a linear wiggler is straightforward.[6]

Statistically averaging over an ensemble of wigglers, it is possible to determine the mean-square centroid motion[6]

$$\langle \delta\beta_x^2 \rangle = D\left(z + \frac{\sin 2k_\beta z}{2k_\beta}\right) \tag{2a}$$

$$\langle \delta x^2 \rangle = \frac{D}{k_\beta^2}\left(z - \frac{\sin 2k_\beta z}{2k_\beta}\right), \tag{2b}$$

where $D = a_w^2 k_w^2 \langle \delta\hat{B}_y^2 \rangle z_{ac}/(2\gamma^2)$. Physically, the centroid orbits δx and $\delta\beta_x$ represent diffusing betatron orbits characterized by a diffusion coefficient D. Notice that by increasing

k_β^2 by additional external focusing, one may, in principle, keep δx_{rms} as small as desired. Furthermore, notice that in the 1D limit, $(2k_\beta z)^2 << 1$, $\langle\delta\beta_z^2\rangle = 2Dz$ and $\langle\delta x^2\rangle = 2Dz^3/3$. Hence, weak focusing (finite k_β) is effective in reducing the asymptotic scaling of the random walk δx_{rms} from $z^{3/2}$ to $z^{1/2}$. To avoid loss of optical guiding it is desirable to keep $\langle\delta x^2\rangle << r_s^2$, where r_s is the radiation spot size.

3. Variations in the Parallel Beam Energy

Not only do the field errors perturb the perpendicular motion of the electrons, they also perturb the parallel motion. This is true since a static magnetic field conserves total electron energy. The parallel motion may easily be calculated[6] using the above expressions for the perpendicular motion along with $\beta_\parallel^2 + \beta_\perp^2$ =constant. One may calculate various statistical moments of the parallel motion,[6] such as the mean parallel energy variation $\langle\delta\gamma_\parallel\rangle = \langle\gamma_\parallel\rangle - \gamma_{\parallel 0}$,

$$\frac{\langle\delta\gamma_\parallel\rangle}{\gamma_{\parallel 0}} = -\frac{(1 + a_w^2/4)}{(1 + a_w^2)^2}a_w^2 k_w^2 \langle\delta\hat{B}^2\rangle z_{ac} z, \tag{3}$$

where the limit $(2k_\beta z)^2 >> 1$ has been assumed.

Statistically, $\langle\delta\gamma_\parallel\rangle$ may be interpreted as an effective energy spread due to field errors.[6] This effective energy spread may lead to a loss of FEL resonance. Heuristically, in order to maintain resonance, one expects that in the low or high gain regime the effective energy spread must be small compared to the intrinsic FEL efficiency η, $|\langle\delta\gamma_\parallel\rangle|/\gamma_{\parallel 0} < \eta$. In the trapped particle regime, maintaining resonance implies that the effective energy spread must be small compared to the depth of the ponderomotive well, $|\langle\delta\gamma_\parallel\rangle|/\gamma_{\parallel 0} < |e\Phi_p|/(\gamma mc^2)$, where Φ_p is the ponderomotive potential. For example, in the low gain regime, $\eta = 1/(2N)$. The inequality $|\langle\delta\gamma_\parallel\rangle|/\gamma_{\parallel 0} < \eta$ implies $\delta\hat{B}_{rms} < 1/(\pi N) \simeq 0.3\%$ for $N = 100$ (where $a_w^2 >> 1$ has been assumed).

4. Deviations in the Relative Phase

To quantify how the parallel energy variation affects FEL gain, it is necessary to consider the relative phase ψ of the electrons in the ponderomotive wave, $d\psi/dz \equiv k + k_w - \omega/(c\beta_z)$. In the small signal limit ($a_R \to 0$, where a_R is the normalized radiation field), the deviation in phase $\delta\psi$ due to the field errors is given by

$$\delta\psi = -\frac{\omega}{2c}\int_0^z dz'(2\beta_{\perp 0}\delta\beta_\perp + \delta\beta_\perp^2), \tag{4}$$

3

where $\beta_{\perp 0}$ is the ideal wiggle motion (in the absence of field errors) and where $\delta\beta_{\perp}$ is given by Eq. (1a). Statistically averaging over the wiggler ensemble gives

$$\langle \delta\psi \rangle = -\frac{a_w^2 k_w^3}{(1 + a_w^2)} \langle \delta\tilde{B}^2 \rangle \frac{z_{ac}}{2} \left[\frac{z^2}{2} + \frac{1}{4k_\beta^2} (1 - \cos 2k_\beta z) \right]. \tag{5}$$

Notice that $\langle \delta\psi \rangle \simeq C_0 z^2/2$ in the limit $(2k_\beta z)^2 \gg 1$; and $\langle \delta\psi \rangle \simeq C_0 z^2$ in the limit $(2k_\beta z)^2 \ll 1$. Hence, transverse focusing only reduces $\langle \delta\psi \rangle$ by 1/2. It should be mentioned that in the trapped particle regime, the effects of the synchrotron motion of the electrons may further reduce[4] $\langle \delta\psi \rangle$.

Physically, $\delta\psi$ may be interpreted as an oscillation of the ponderomotive well due to field errors. Maintaining FEL resonance requires $\delta\psi$ to be small compared to π, i.e., the width of the well. In the low gain regime, this phase deviation must be kept small over the entire wiggler length L. Requiring $|\langle \delta\psi(z = L) \rangle| < \pi$ implies $\delta\tilde{B}_{rms} < 1/(\pi N) \sim 0.3\%$ for $N = 100$ (where $a_w^2 \gg 1$ has been assumed). This is the same condition as obtained above from considering the effective energy spread. In the high gain regime, the situation is somewhat different, since the length scale over which the FEL resonant interaction occurs is the e–folding length $1/\Gamma$, where Γ is the spatial growth rate of the radiation. Maintaining resonance in the high gain regime corresponds to keeping $\delta\psi$ small over an e–folding length: $|\langle \delta\psi(z = 1/\Gamma) \rangle| < \pi$. Since, typically $1/\Gamma \ll L$, one expects the high gain not to be strongly affected by the phase deviation $\delta\psi$ (in contrast to the low gain).

5. Degradation of FEL Gain

Quantitatively, the effect of the phase deviation on the FEL gain in the low gain regime may be determined analytically. The normalized mean amplitude gain is related to $\delta\psi$ by the following expression,

$$\langle \hat{G} \rangle = \int_0^z dz' \int_0^{z'} dz''(z' - z'') \langle \sin[\mu k_w(z' - z'') + \Delta\delta\psi] \rangle, \tag{6}$$

where $\Delta\delta\psi \equiv \delta\psi(z') - \delta\psi(z'')$ and μ = normalized frequency mismatch. Setting $\Delta\delta\psi = 0$ in the above equation gives the gain in the absence of field errors.

Evaluation of the ensemble average in the above expression is dependent on the statistical distribution of the function $\Delta\delta\psi$. Recall that the phase deviation $\delta\psi$ is proportional to terms which are linear in the field error δB as well as terms which are quadratic in the field error, as indicated by Eq. (4). If the field error δB is a Gaussian distributed

random variable, then terms quadratic in δB tend to obey a Gamma distribution. Hence, if the quadratic terms dominate in the expression for $\delta\psi$, then $\delta\psi$ will tend to be Gamma distributed. Assuming $\Delta\delta\psi$ to be approximately Gamma distributed allows the ensemble average in Eq. (6) to be evaluated using the Rice–Mandel approximation,[2,9] yielding

$$
\langle\hat{G}\rangle = \int_0^z dz' \int_0^{z'} dz''(z' - z'')\left(1 + \langle\Delta\delta\psi\rangle^2/f^2\right)^{-f/2}
$$
$$
\times \sin\left[\mu k_w(z' - z'') + f\tan^{-1}\left(\langle\Delta\delta\psi\rangle/f\right)\right], \tag{7}
$$

where $f = \langle\Delta\delta\psi\rangle^2/\left(\langle\Delta\delta\psi^2\rangle - \langle\Delta\delta\psi\rangle^2\right)$.

It is possible to show that the mean gain is a function of only two parameters, $\langle\hat{G}\rangle = F(\mu, \langle\delta\psi\rangle_{max})$, where $\langle\delta\psi\rangle_{max} = \langle\delta\psi(z = L)\rangle$. Furthermore, one can show that $\langle\hat{G}\rangle$ decreases as $\langle\delta\psi\rangle_{max}$ increases. In a similar fashion, it is possible to calculate expressions for the variance of the gain. This variance tends to be large, as is indicated by the numerical simulations discussed below.

Equation (7) may be evaluated numerically to determine the behavior of the mean gain. Figure 1 illustrates this behavior, in which the mean gain $\langle\hat{G}\rangle$ is plotted as a function of the frequency mismatch μ for several values of rms field error $\delta\hat{B}_{rms}$. The parameters in Fig. 1 correspond to a linearly polarized wiggler with $B_w = 5.4$ kG, $\lambda_w = 2.8$ cm, $L = 3.6$ m and $\gamma = 350$ in the limit $k_\beta = 0$ (transverse focusing is neglected). Figure 2 shows the peak gain $\langle\hat{G}\rangle_{max}$ as a function of rms field error $\delta\hat{B}_{rms}$. In Fig. 2, the solid line shows the solution to Eq. (6) in which the ensemble average is evaluated numerically (assuming a uniform distribution of field errors between $\pm\delta B_{max}$), whereas the dashed curve shows the solution to Eq. (7) in which the ensemble average is evaluated using the Rice–Mandel approximation. The circles in Fig. 2 are the result of an FEL simulation code for individual wiggler realizations (particular arrangements of random field errors). In these simulation runs, a random field error model similar to that of Kincaid[2,6–8] was used along with an electron beam of current 2.0 A with an emittance of 10 μm-rad. Notice that the large spread in the simulation results indicates a relatively large variance of the gain.

It is also possible to calculate the effect of wiggler errors on the spatial growth rate in the high gain regime.[7] Figure 3 shows the numerically evaluated spatial growth rate Γ (normalized to the value in the absence of field errors) as a function of the rms field error $\delta\hat{B}_{rms}$. In Fig. 3, the solid points indicate the mean growth rate and the error bars indicate one standard deviation about that mean. These results are for a linearly polarized wiggler with $B_w = 2.4$ kG, $\lambda_w = 8.0$ cm and $L = 15$ m; and for an electron beam of energy 50 MeV with a current of 1.5 kA and an emittance of 4.4 μm-rad. Notice that even for large

5

rms field errors, $\delta\hat{B}_{rms} = 0.5\%$, the mean spatial growth rate is only slightly reduced (by $< 4\%$). This is in agreement with the discussion presented in the previous section.

6. Beam Steering

One method for reducing the detrimental effects of field errors is through the use of beam steering[2-8] (external fields are used to steer the electron beam back to axis). Analytically, this may be modeled by injecting the electron beam with an initial perpendicular velocity $\beta_{\perp 0}$ such that the centroid displacement is zero at the end of the wiggler $\delta x(z = L) = 0$. The intial perpendicular velocity may be specified in terms of the perturbed perpendicular velocity in the absence of steering $\delta\beta_{\perp N}$ by the relation

$$\beta_{\perp 0} = -\frac{1}{L}\int_0^L dz' \delta\beta_{\perp N}(z'),\tag{8}$$

where $\delta B_{\perp N}$ is given by Eq. (1a).

Using the above expression for $\beta_{\perp 0}$, one may calculate the electron motion in the presence of the field errors including the effects of beam steering. For example, the phase deviation in the absence of transverse focusing ($k_\beta = 0$) is given by

$$\langle\delta\psi\rangle = -\gamma_{\|0}^2 k_w D\left[z^2 + \epsilon\frac{2}{3}zL\left(1 - \frac{3z}{L} + \frac{z^2}{L^2}\right)\right].\tag{9}$$

where $\epsilon = 1$ with steering and 0 without steering and where $\gamma_{\|0}$ is the parallel relativistic factor in the absence of field errors. In particular, notice that the effect of steering is to reduce the mean phase deviation by a factor of 1/3, $\langle\delta\psi(L, \epsilon = 1)\rangle = (1/3)\langle\delta\psi(L, \epsilon = 0)\rangle$. It is also possible to calculate $\langle\hat{G}\rangle$ including the effects of steering.

The effect of beam steering at the wiggler entrance on the phase deviation $\delta\psi$ is illustrated in Fig. 4 for the cases (a) without steering and (b) with steering. Here the solid curves represent the mean $\langle\delta\psi\rangle$ and the dashed curves represent one standard deviation about the mean $\langle\delta\psi\rangle \pm \sigma$, where σ is the variance of the phase deviation. These plots are for a linearly polarized wiggler with $B_w = 5.4$ kG. $\lambda_w = 2.8$ cm. $L = 3.6$ m. $\gamma = 350$ and $\delta\hat{B}_{rms} = 0.3\%$ in the limit $k_\beta = 0$ (transverse focusing is neglected). Notice that the effect of steering at the wiggler entrance reduces $\langle\delta\psi\rangle$ by 1/3 at the end of the wiggler, as is indicated by Eq. (9). Also, notice that steering has reduced the variance of the phase deviation by an equally significant amount. For cases in which $k_\beta \neq 0$, it is possible to show[8] that steering reduces the mean phase deviation when the length over which the

6

steering in performed is less than the betatron wavelength, $L_s < \lambda_\beta$. For cases in which $L_s > \lambda_\beta$, beam steering may increase the value of $\langle \delta \psi \rangle$.

The effect of beam steering at the wiggler entrance on the FEL gain (in the low gain regime) is illustrated in Fig. 5. Here the peak normalized gain $\langle \hat{G} \rangle_{max}$ is plotted as a function of the rms field error $\hat{\delta B}_{rms}$ for the case with steering and for the case with no steering. The parameters in Fig. 5 correspond to a linearly polarized wiggler with $B_w = 5.4$ kG, $\lambda_w = 2.8$ cm, $L = 1.8$ m and $\gamma = 350$ in the limit $k_\beta = 0$. Figure 5 indicates that the mean gain may be significantly enhanced by using steering at the wiggler entrance.

7. Error Reduction Techniques

Several methods exist for reducing the detrimental effects of wiggler errors. Above it was discussed how steering[2-8] the electron beam at the entrance of the wiggler may improve FEL performance. This concept may be generalized to the case of multiple beam steering,[3,4,8] in which the electron beam is steered back to axis in several places along the length of the wiggler. In addition to beam steering, one may consider wiggler errors which are correlated.[8] The results discussed above are for wigglers with random errors which are assumed to be uncorrelated for separation distances greater than $z_{ac} \simeq \lambda_w/2$. By considering a wiggler in which the error for a given magnet pole is correlated to the errors of the surrounding poles, one may construct beneficial correlations which reduce the detrimental effects of the errors.

Alternatively, one may reduce the detrimental effects of the errors by considering an optimal arrangement of the magnet poles.[10-12] That is, the magnet poles are to be arranged in such a way that the detrimental effects of the error of a given pole tend to cancel those of the surrounding poles. More specifically, the magnet poles are arranged in such a way as to minimize an appropriate "cost function". For example, one may choose to arrange the poles such that the magnitude of random walk $|\delta x|$ is minimized, where $\delta x \sim \int dz' \sin k_\beta(z' - z)\delta\hat{B}_y(z')$. (Notice that minimization of $|\int dz \delta B|$ does not correspond to minimization of $|\delta x|$.) However, the results discussed above indicate that a more appropriate cost function is the magnitude of the phase deviation $|\delta\psi|$, $\delta\psi \sim \int dz'(2\beta_{\perp 0}\delta\beta_\perp + \delta\beta_\perp^2)$, where $\delta\beta_z \sim \int dz' \cos k_\beta(z' - z)\delta\hat{B}_y(z')$. By minimizing $|\delta\psi|$, one reduces the amount of gain loss. Ideally, one would like to maximize the actual expression for the gain, Eq. (6), but the functional dependence of the gain on the field errors appears much too complicated to be of practical usefulness.

8. Conclusions

The analytical and numerical work discussed above indicates that the the phase deviation $\delta\psi$ is the single most important parameter characterizing the effects of wiggler errors. Although transverse beam focusing and beam steering are highly effective in controlling the random walk δx (in principle, δx may be kept as small as desired), this is not the case for the phase deviation $\delta\psi$. Transverse beam focusing only reduces the mean phase deviation by a factor of $1/2$, $\langle\delta\psi\rangle = (1/2)\langle\psi(k_\beta = 0)\rangle$. Beam steering may be used to reduce $|\delta\psi|$ only when $L_S < \lambda_\beta$. As an example, for the case $k_\beta = 0$ and using steering at the wiggler entrance indicates that the mean phase deviation at the wiggler end is reduced by a factor of $1/3$, $\langle\delta\psi(\epsilon = 1)\rangle = (1/3)\langle\delta\psi(\epsilon = 0)\rangle$. The phase deviation leads to a reduction of FEL gain (the low gain regime is affected more strongly than the high gain regime). To avoid significant loss in gain, the above analysis implies that $|\langle\delta\psi\rangle| < \pi$. In the low gain regime, this gives

$$\delta\hat{B}_{rms} < \alpha/(\pi N), \tag{10}$$

where $\alpha = (1 + a_w^2)^{1/2}/a_w$ for a helical wiggler. Possible error reduction techniques include multiple beam steering, correlation of field errors and optimal arrangement of magnet poles. An optimal arrangement of poles corresponds to minimization of $|\delta\psi|$, where $\delta\psi$ is given by Eq. (4).

Acknowledgements

References

1) K.E. Robinson, D.C. Quimby and J.M. Slater, IEEE J. Quantum Electron. **QE-23**, 1497 (1987); K.E. Robinson, D.C. Quimby, J.M. Slater, T.L. Churchill and A.S. Valla, Nucl. Instr. and Meth. **A259**, 62 (1987).

2) B.M. Kincaid, J. Opt. Soc. Am. B **2**, 1294 (1985).

3) C.J. Elliott and B.D. McVey, in *World Sci. Proc. Undulator Magnets for Synchrotron Radiation and Free Electron Lasers*, Trieste, Italy (1987).

4) H.D. Shay and E.T. Scharlemann, Nucl. Instr. and Meth. **A272**, 601 (1988).

5) E. Esarey, W. Marabl , C.M. Tang and P. Sprangle, Bull. Am. Phys. Soc. **33**, 1066 (1988).

6) E. Esarey, W. Marable and C.M. Tang, NRL Memo. Report 6523 (1989); submitted to J. Appl. Phys.

7) W. Marable, E. Esarey and C.M. Tang, submitted to Phys. Rev. A.

8) W. Marable, E. Esarey and C.M. Tang, submitted to Phys. Fluids; these Proceedings (11th Intl. FEL Conf., Naples, FL, 1989).

9) S.O. Rice, Bell Syst. Tech. J. **24**, 46 (1945); L. Mandel, Proc. Phys. Soc. **74**, 233 (1959).

10) A. Cox and B. Youngman, Proc. SPIE **582**, 91 (1986).

11) G. Rakowsky, B. Bobbs and D.C. Slater, Bull. Am. Phys. Soc. **33**, 908 (1988).

12) M.S. Curtin, A. Bhowmik, W.A. McMullin, S.V. Benson, J.M.J. Madey, B.A. Richman and L. Vintro, Nucl. Instr. and Meth. **A272**, 91 (1988).
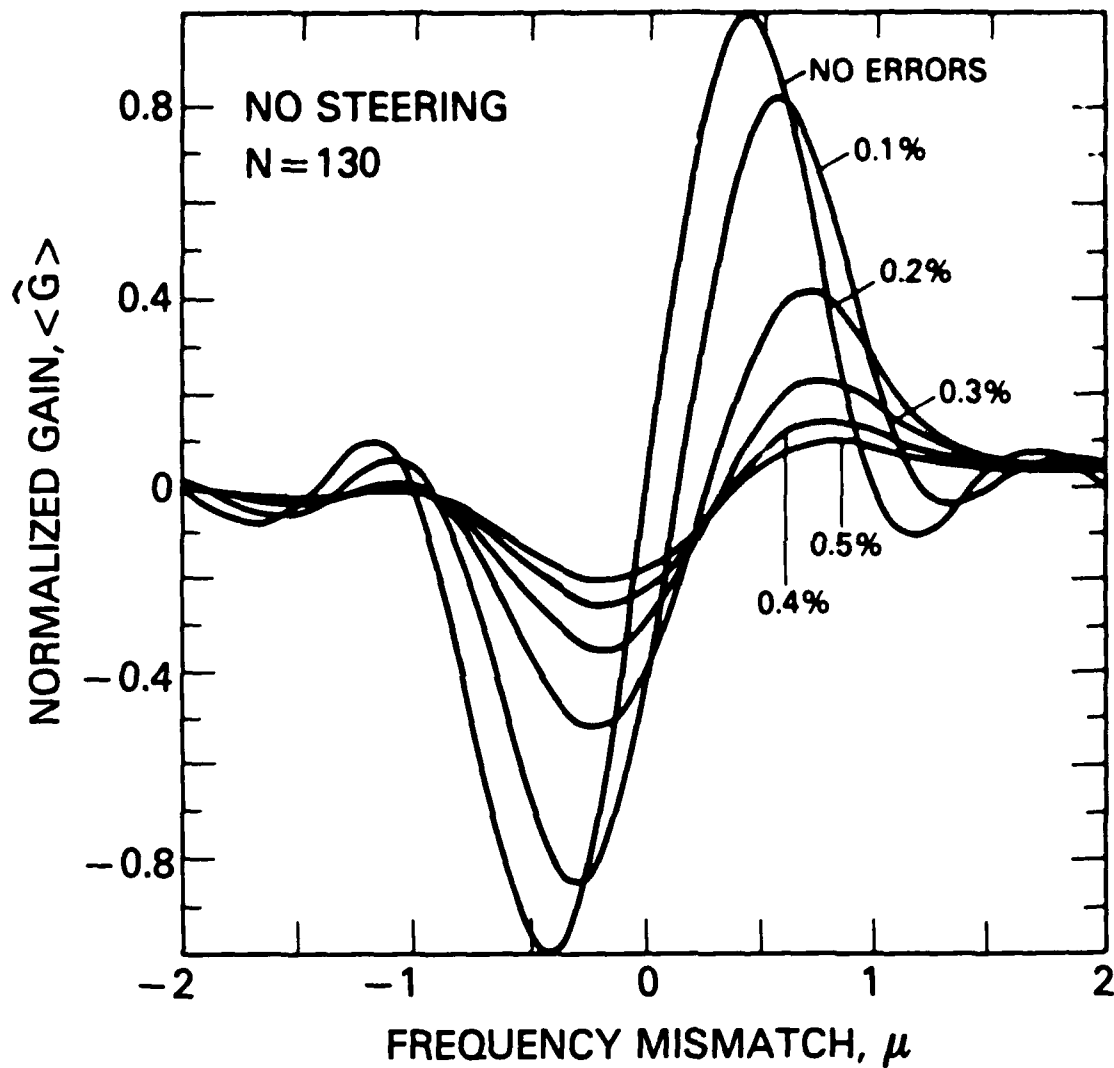
Fig. 1. Mean gain $\langle \hat{G} \rangle$ versus frequency mismatch μ for several values of rms field error $\delta \hat{B}_{rms}$ for a linearly polarized wiggler with $B_w = 5.4$ kG, $\lambda_w = 2.8$ cm, $L = 3.6$ m and $\gamma = 350$ in the limit $k_\beta = 0$.
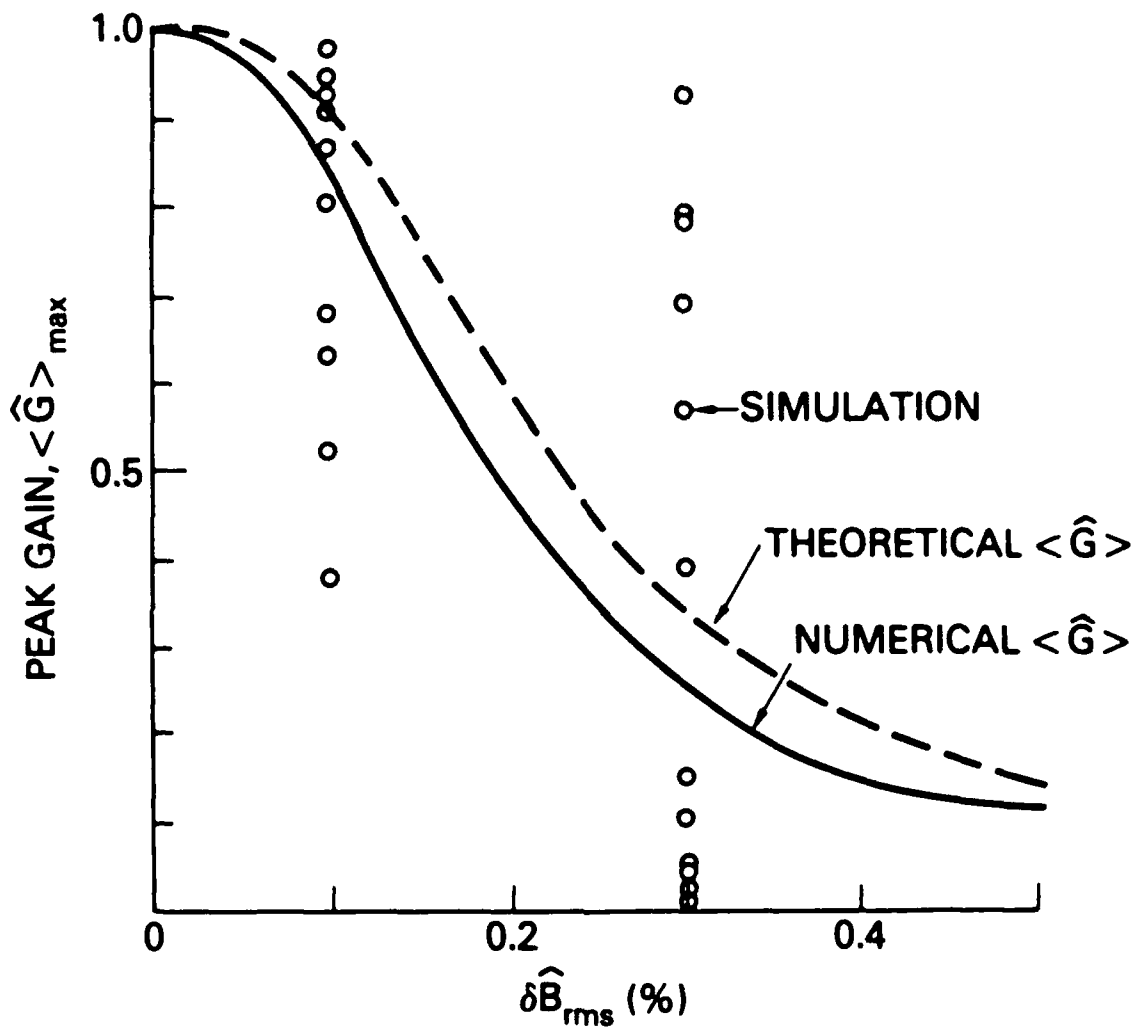
Fig. 2. Peak mean gain $\langle \hat{G} \rangle_{max}$ versus rms field error $\delta \hat{B}_{rms}$ for a linearly polarized wiggler with $B_w = 5.4$ kG, $\lambda_w = 2.8$ cm, $L = 3.6$ m and $\gamma = 350$ in the limit $k_\beta = 0$. The solid curve denotes a numerical average, the dashed curve denotes a theoretical average and the circles denote FEL simulations.

11
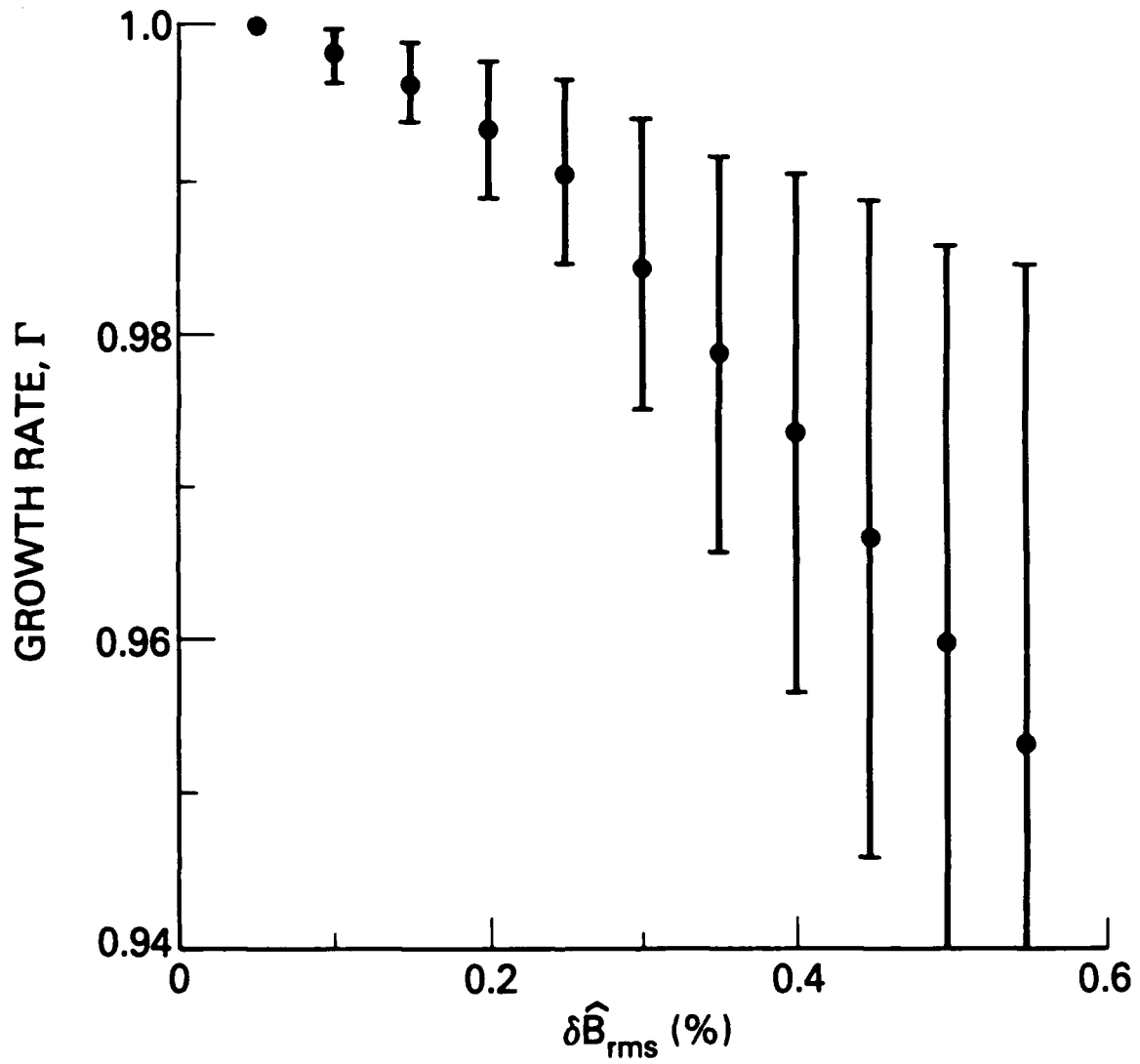
Fig. 3. High gain spatial growth rate Γ versus rms field error $\delta\hat{B}_{rms}$ for a linearly polarized wiggler with $B_w = 2.4$ kG, $\lambda_w = 8.0$ cm and $L = 15$ m and $\gamma = 100$. The solid points denote the mean and the error bars denote one standard deviation.
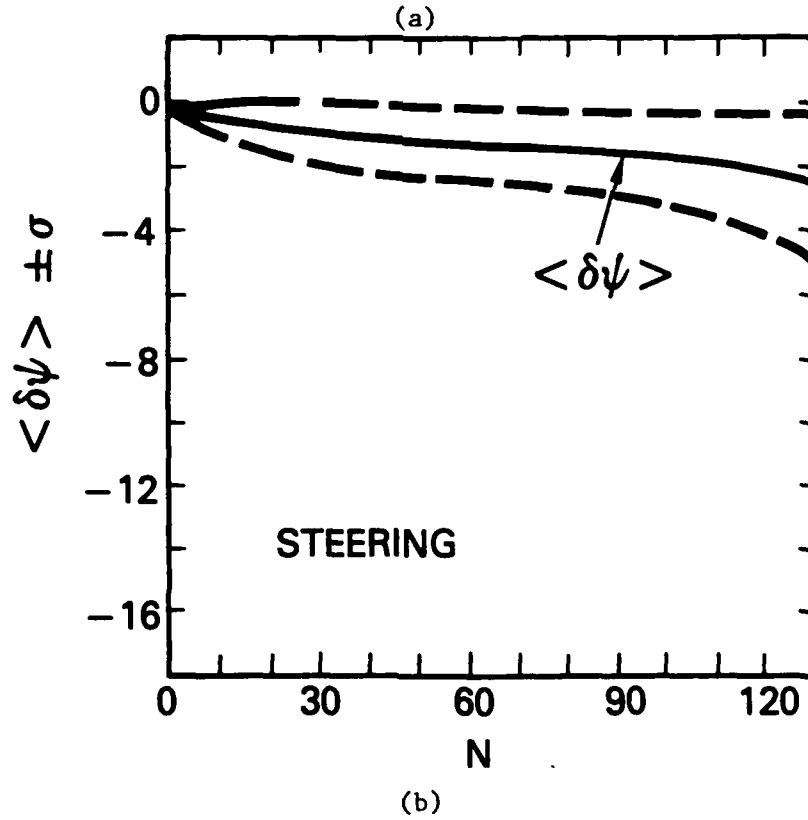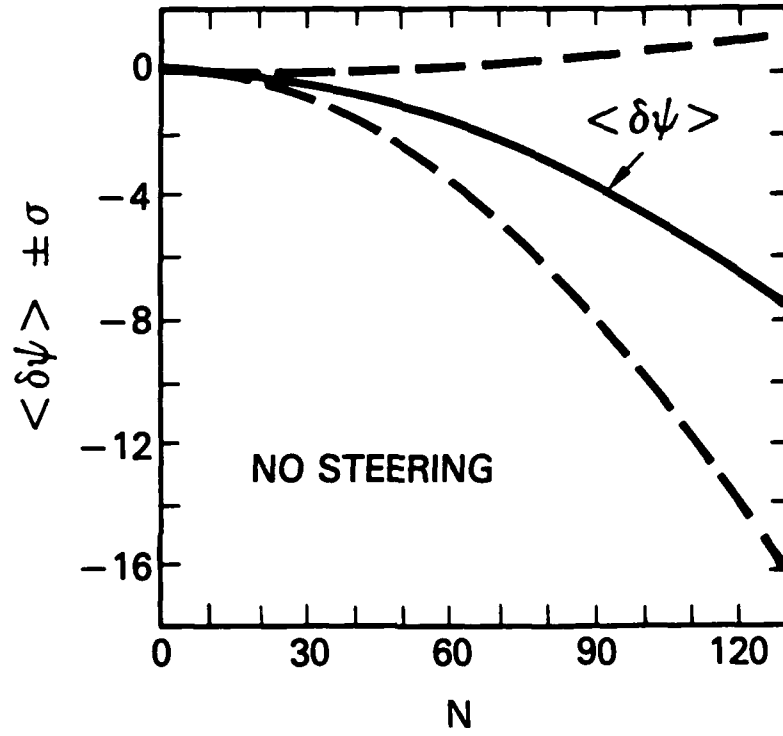
Fig. 4. Phase deviation $\delta\psi$ versus number of wiggler periods N (a) without steering and (b) with steering for a linearly polarized wiggler with $B_w = 5.4$ kG, $\lambda_w = 2.8$ cm, $L = 3.6$ m, $\gamma = 350$ and $\delta\hat{B}_{rms} = 0.3\%$ in the limit $k_\beta = 0$. The solid curves represent the mean $\langle\delta\psi\rangle$ and the dashed curves represent one standard deviation σ about the mean.

13
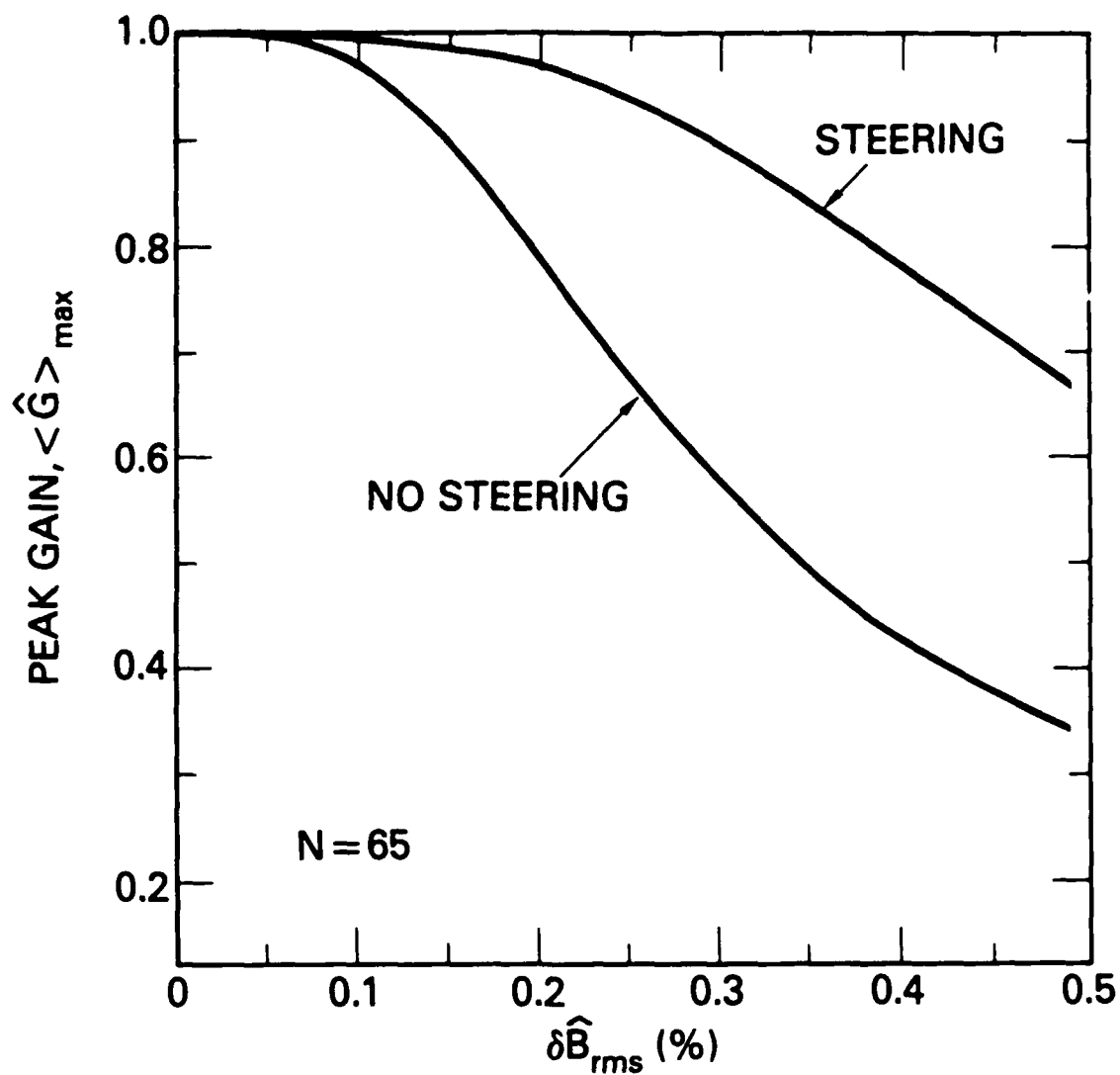
Fig. 5. Peak gain $\langle \hat{G} \rangle_{max}$ versus rms field error $\delta \hat{B}_{rms}$ with and without steering for a linearly polarized wiggler with $B_w = 5.4$ kG, $\lambda_w = 2.8$ cm, $L = 1.8$ m and $\gamma = 350$ in the limit $k_\beta = 0$.

DISTRIBUTION LIST

Naval Research Laboratory
4555 Overlook Avenue, S.W.
Washington, DC 20375-5000
       Attn: Code 1000 - Commanding Officer, CAPT John J. Donegan, Jr.
                    1001 - Dr. T. Coffey
                    1005 - Head, Office of Management & Admin.
                    1005.1-Deputy Head, Office of Management & Admin.
                    1005.6-Head, Directives Staff
                    1200 - CAPT R. W. Michaux
                    1201 - Deputy Head, Command Support Division
   1220 - Mr. M. Ferguson
                    2000 - Director of Technical Services
                    2604 - NRL Historian
                    3000 - Director of Business Operations
                    4000 - Dr. W. R. Ellis
                    0124 - ONR
                    4600 - Dr. D. Nagel
                    4603 - Dr. W. W. Zachary
                    4700 - Dr. S. Ossakow (26 copies)
                    4700.1-Dr A. W. Ali
                    4790 - Dr. P. Sprangle
                    4790 - Dr. C. A. Kapetanakos
                    4790 - Dr. J. Mathew
                    4730 - Dr. R. Elton
                    4707 - Dr. W. M. Manheimer
                    4790 - Dr. W. Black
                    4790 - Dr. A. W. Fliflet
                    4790 - Dr. S. Gold
                    4790 - Dr. D. L. Hardesty
                    4790 - Dr. A. K. Kinkead
                    4790 - Dr. M. Rhinewine
                    4770 - Dr. G. Cooperstein
                    4790 - Dr. C. M. Tang (25 copies)
                    4790 - Dr. G. Joyce
                    4790 - Dr. M. Lampe
                    4790 - Dr. Y. Y. Lau
                    4790 - Dr. A. Ting
                    4790 - Dr. E. Esarey (25 copies)
                    4790 - Dr. J. Krall
                    4790A- B. Pitcher (10 copies)
                    5700 - Dr. L. A. Cosby
                    5745 - Dr. J. Condon
                    6840 - Dr. S. Y. Ahn
                    6840 - Dr. A. Ganguly
                    6840 - Dr. R. K. Parker
                    6843 - Dr. R. H. Jackson
                    6843 - Dr. N. R. Vanderplaats
                    6843 - Dr. C. M. Armstrong
                    6875 - Dr. R. Wagner
                    2628 - Documents (22 copies)
                    2634 - D. Wilbanks
NOTE: Every name listed on distribution gets one copy except for those
where extra copies are noted.

15

Dr. R. E. Aamodt
Lodestar Research Corp.
2400 Central Ave., P-5
Boulder, CO 80306-4545

Dr. J. Adamski
Boeing Aerospace Company
P.O. Box 3999
Seattle, WA 98124

Dr. T. M. Antonsen
University of Maryland
College Park, MD 20742

Assistant Secretary of the
Air Force (RD&L)
Room 4E856, The Pentagon
Washington, D.C. 20330

Dr. W. A. Barletta
Lawrence Livermore National Lab.
P. O. Box 808
Livermore, CA 94550

Dr. W. Becker
Univ. of New Mexico
Institute for Mod. Opt.
Albuquerque, NM 87131

Dr. Robert Behringer
9342 Balcon Ave.
Northridge, CA 91325

Dr. G. Bekefi
Mass. Institute of Tech.
Room 36-213
Cambridge, MA 02139

Dr. Steven V. Benson
Physics Building
Duke University
Durham, NC 27706

Dr. I. B. Bernstein
Mason Laboratory
Yale University
400 Temple Street
New Haven, CT 06520

Dr. Amitava Bhattacharjee
Columbia University
S. W. Mudd 210
Dept. of Applied Phys.
New York, NY 10027

Dr. Anup Bhowmik
Rockwell International/Rocketdyne Div.
6633 Canoga Avenue, FA-40
Canoga Park, CA 91304

Dr. G. Bourianoff
1901 Rutland Drive
Austin, TX 78758

Dr. Charles Brau
Vanderbilt University
Nashville, TN 37235

Dr. R. Briggs
SSC Laboratory
Stoneridge Office Park
2550 Beckleymeade Ave.
Suite 260
Dallas, TX 75237

Prof. William Case
Dept. of Physics
Grinnell College
Grinnell, IA 50112

Dr. R. Center
Spectra Tech., Inc.
2755 Northup Way
Bellevue, WA 98004

Dr. K. C. Chan
Los Alamos National Laboratory
P. O. Box 1663
Los Alamos, NM 87545

Prof. Frank Chen
School of Eng. & Applied Sciences
Univ. of Calif. at Los Angeles
7731 K Boelter Hall
Los Angeles, CA 90024

Dr. S. Chen
MIT Plasma Fusion Center
NW16-176
Cambridge, MA 01890

Dr. D. P. Chernin
Science Applications Intl. Corp.
1720 Goodridge Drive
McLean, VA 22102

Dr. William Colson
Berkeley Research Assoc.
P. O. Box 241
Berkeley, CA 94701

Dr. Richard Cooper
Los Alamos National Scientific
Laboratory
P.O. Box 1663
Los Alamos, NM 87545

Dr. R. A. Cover
Rockwell International/Rocketdyne Div.
6633 Canoga Avenue, FA-38
Canoga Park, CA 91304

Dr. Bruce Danly
MIT
NW16-174
Cambridge, MA 02139

Dr. R. Davidson
Plasma Fusion Center
Mass. Institute of Tech.
Cambridge, MA 02139

Dr. John Dawson
Physics Department
University of California
Los Angeles, CA 90024

Dr. David A. G. Deacon
Deacon Research
Suite 203
900 Welch Road
Palo Alto, CA 94304

Dr. Philip Debenham
Center for Radiation Research
National Bureau of Standards
Gaithersburg, MD 20899

Director
National Security Agency
Fort Meade, MD 20755
ATTN: Dr. Richard Foss, A42
       Dr. Thomas Handel, A243
       Dr. Robert Madden, R/SA

Director of Research (2 copies)
U. S. Naval Academy
Annapolis, MD 21402

Dr. A. Drobot
Science Applications Intl. Corp.
1710 Goodridge Road
McLean, VA 22102

Dr. Dwight Duston
SDIO/IST
The Pentagon
Washington, DC 20301-7100

Dr. Luis R. Elias
Creol-FEL Research Pavillion
Suite 400
12424 Research Parkway
Orlando, FL 32826

Dr. C. James Elliott
X1-Division, M.S. 531
Los Alamos Natl. Scientific Lab.
P. O. Box 1663
Los Alamos, NM 87545

Dr. Anne-Marie Fauchet
Brookhaven National Laboratories
Associated Universities, Inc.
Upton, L.I., NY 11973

Dr. R. Gajewski
Div. of Advanced Energy Projects
U. S. Dept of Energy
Washington, DC 20545

Dr. J. Gallardo
Brookhaven National Laboratory
Associated Universities, Inc.
Upton, L.I., NY 11973

Dr. B. B. Godfrey,
Chief Scientist
WL/CA
Kirtland AFB, NM 87117-6008

Dr. John C. Goldstein, X-1
Los Alamos Natl. Scientific Lab.
P.O. Box 1663
Los Alamos, NM 87545

Dr. V. L. Granatstein
Dept. of Electrical Engineering
University of Maryland
College Park, MD 20742

Dr. K. Halbach
Lawrence Berkeley Laboratory
University of California, Berkeley
Berkeley, CA 94720

Dr. R. Harvey
Hughes Research Laboratory
3011 Malibu Canyon Road
Malibu, CA 90265

Prof. Herman A Haus
Mass. Institute of Technology
Rm. 36-351
Cambridge, MA 02139

Dr. B. Hui
Defense Advanced Research Projects Agency
1400 Wilson Blvd.
Arlington, VA 22209

Prof. V. Jaccarino
Univ. of Calif. at Santa Barbara
Santa Barbara, CA 93106

Dr. B. Carol Johnson
Ctr. for Radiation Research
National Inst. of Standards and Tech.
Gaithersburg, MD 20899

Dr. Ron Johnson
Ctr. for Radiatiuon Research
Natl. Inst. of Standards and Tech.
Gaithersburg, MD 20899

Dr. Shayne Johnston
Physics Department
Jackson State University
Jackson, MS 39217

Dr. R. A. Jong
Lawrence Livermore National Laboratory
P. O. Box 808/L626
Livermore, CA 94550

Dr. Howard Jory
Varian Associates, Bldg. 1
611 Hansen Way
Palo Alto, CA 94303

Dr. C. Joshi
University of California
Los Angeles, CA 90024

Dr. K. J. Kim, MS-101
Lawrence Berkeley Lab.
Rm. 223, B-80
Berkeley, CA 94720

Dr. Brian Kincaid
Lawrence Berkeley Laboratory
University of California, Berkeley
Berkeley, CA 94720

Prof. N. M. Kroll
Department of Physics
B-019, UCSD
La Jolla, CA 92093

Dr. Thomas Kwan
Los Alamos National Scientific
Laboratory, MS608
P. O. Box 1663
Los Alamos, NM 87545

Dr. J. LaSala
Physics Dept.
U. S. M. A.
West Point, NY 10996

Dr. Michael Lavan
U.S. Army Strategic Def. Command
ATTN: Code CSSD-H-D
P. O. Box 1500
Huntsville, AL 35807-3801

Dr. B. Levush
Dept. of Physics & Astronomy
University of Maryland
College Park, MD 20742

Dr. Anthony T. Lin
Dept. of Physics
University of California
Los Angeles, CA 90024

Dr. Chuan S. Liu
Dept. of Physics & Astronomy
University of Maryland
College Park, MD 20742

Dr. A. Luccio
Brookhaven National Laboratory
Accelerator Dept.
Upton, NY 11973

Prof. J.M.J. Madey
117 Physics Bldg.
Duke University
Durham, NC 27706

Dr. R. Mako
205 South Whiting Street
Alexandria, VA 22304

Dr. Joseph Mangano
Science Research Laboratory
1600 Wilson Blvd.
Suite 1200
Arlington, VA 22209

Dr. Siva A. Mani
Science Applications Intl. Corp.
1040 Waltham Street
Lexington, MA 02173-8027

Dr. T. C. Marshall
Applied Physics Department
Columbia University
New York, NY 10027

Dr. Xavier K. Maruyama
Dept. of Physics
Naval Postgraduate School
Monterey, CA 93943

Dr. B. McVey
Los Alamos National Laboratory
P. O. Box 1663
Los Alamos, NM 87545

Dr. David Merritt
Space & Naval Warfare Command
Attn: PMW 145A
Washington, DC 20363-5100

Dr. A. Mondelli
Science Applications Intl. Corp.
1710 Goodridge Drive
P.O. Box 1303
McLean, VA 22101

Dr. Mel Month
Brookhaven National Laboratories
Associated Universities, Inc.
Upton, L.I., NY 11973

Dr. Gerald T. Moore
University of New Mexico
Albuquerque, NM 87131

Dr. Philip Morton
Stanford Linear Accelerator Center
P.O. Box 4349
Stanford, CA 94305

Prof. J. Nation
224 Phillips Hall
School of Elec. Eng.
Cornell University
Ithaca, NY 14850

Dr. George Neil
TRW
One Space Park
Redondo Beach, CA 90278

Dr. Kelvin Neil
Lawrence Livermore National Lab.
Code L-321, P.O. Box 808
Livermore, CA 94550

Dr. Brian Newnam
MSJ 564
Los Alamos National Scientific Lab.
P.O. Box 1663
Los Alamos, NM 87545

Dr. T. Orzechowski
L-436
Lawrence Livermore National Lab.
P. O. Box 808
Livermore, CA 94550

Prof. E. Ott
Department of Physics
University of Maryland
College Park, MD 20742

OUSDRE (R&AT)
Room 3D1067, The Pentagon
Washington, D.C. 20301

Dr. Robert B. Palmer
Brookhaven National Laboratories
Associated Universities, Inc.
Upton, L.I., NY 11973

Dr. J. Palmer
Hughes Research Laboratory
Malibu, CA 90265

Dr. Richard H. Pantell
Stanford University
Stanford, CA 94305

Dr. Dennis Papadopoulos
Astronomy Department
University of Maryland
College Park, Md. 20742

Dr. John A. Pasour
Mission Research Laboratory
8560 Cinderbed Road
Suite 700
Newington, VA 22122

Dr. C. K. N. Patel
Bell Laboratories
Murray Hill, NJ 07974

Dr. Claudio Pellegrini
Brookhaven National Laboratory
Associated Universities, Inc.
Upton, L.I., NY 11973

Dr. S. Penner
Center for Radiation Research
Natl. Inst. of Standards and Tech.
Gaithersburg, MD 20899

Dr. M. Piestrup
Adelphi Technology
13800 Skyline Blvd. No. 2
Woodside, CA 94062

Dr. D. J. Pistoresi
Boeing Aerospace Company
P. O. Box 3999
Seattle, WA 98124-2499

Major E. V. Pogue
SDIO
The Pentagon, T-DE Rm. 1E180
Washington, DC 20301-7100

Major Donald Ponikvar
U. S. Army SDC
P. O. Box 15280
Arlington, VA 22245-0280

Dr. Donald Prosnitz
Lawrence Livermore National Lab.
Box 5511 L-626
Livermore, CA 94550

Dr. D. C. Quimby
Spectra Technology
2755 Northup Way
Bellevue, WA 98004

Dr. G. Ramian
Quantum Institute
University of California
Santa Barbara, CA 93106

Dr. M. Reiser
University of Maryland
Department of Physics
College Park, MD 20742

Dr. S. Ride
Arms Control
Stanford University
Stanford, CA 94305

Dr. C. W. Roberson
Office of Naval Research
Code 112S
800 N. Quincy Street
Arlington, VA 22217

Dr. K. Robinson
Spectra Technology
2755 Northup Way
Bellevue, WA 98004

Dr. Marshall N. Rosenbluth
Dept. of Physics
B-019
Univ. of Calif., San Diego
LaJolla, CA 92093

Dr. J. B. Rosenzweig
The Inst. for Accelerator Physics
Department of Physics
University of Wisconsin-Madison
Madison, WI 53706

Dr. N. Rostoker
Department of Physics
University of California at Irvine
Irvine, CA 92717

Dr. A. Saxman
Los Alamos National Scientific Lab.
P. O. Box 1663, MSE523
Los Alamos, NM 87545

Dr. E. T. Scharlemann
L626
Lawrence Livermore National Laboratory
P. O. Box 808
Livermore, CA 94550

Prof. S. P. Schlesinger
Dept. of Electrical Engineering
Columbia University
New York, NY 10027

Dr. Howard Schlossberg
AFOSR
Bolling AFB
Washington, D.C.   20332

Dr. George Schmidt
Stevens Institute of Technology
Physics Department
Hoboken, NJ   07030

Dr. M. J. Schmitt
Los Alamos National Laboratory
P. O. Box 1663
Los Alamos, NM 87545

Dr. H. Schwettmann
Phys. Dept. & High Energy
Physics Laboratory
Stanford University
Stanford, CA   94305

Dr. Marlan O. Scully
Dept. of Physics & Astronomy
Univ. of New Mexico
800 Yale Blvd. NE
Albuquerque, NM   87131

Dr. S. B. Segall
KMS Fusion
3941 Research Park Dr.
P.O. Box 1567
Ann Arbor, MI   48106

Prof. P. Serafim
Northeastern University
Boston, MA   02115

Dr. A. M. Sessler
Lawrence Berkeley Laboratory
University of California
1 Cyclotron Road
Berkeley, CA   94720

Dr. W. Sharp
L-626
Lawrence Livermore National Laboratory
P. O. Box 808
Livermore, CA 94550

Dr. Earl D. Shaw
Bell Laboratories
600 Mountain Avenue
Murray Hill, NJ   07974

Dr. R. L. Sheffield
Los Alamos National Laboratory
P.O. Box 1663
Los Alamos, NM 87545

Dr. D. Shoffstall
Boeing Aerospace Company
P.O. Box 3999
Seattle, WA   98124

Dr. Jack Slater
Spectra Technology
2755 Northup Way
Bellevue, WA   98004

Dr. Todd Smith
Hansen Labs
Stanford University
Stanford, CA   94305

Dr. R. Sudan
Lab. of Plasma Studies
Cornell University
Ithaca, NY   14850

Dr. David F. Sutter
ER 224, GTN
Department of Energy
Washington, D.C.   20545

Dr. T. Tajima
Institute for Fusion Studies
University of Texas at Austin
Austin, TX   78712

Dr. R. Temkin
Mass. Institute of Technology
Plasma Fusion Center
Cambridge, MA   02139

Dr. L. Thode
Los Alamos National Laboratory
P. O. Box 1663
Los Alamos, NM 87545

Dr. Norman H. Tolk
Physics Department
Vanderbilt University
Nashville, TN   37240

Dr. Kang Tsang
Science Applications Intl. Corp.
1710 Goodridge Dr.
McLean, VA 22102

Dr. H. S. Uhm
Naval Surface Warfare Center
White Oak Lab.
Silver Spring, MD   20903-5000

Under Secretary of Defense (R&D)
Office of the Secretary of Defense
Room 3E1006, The Pentagon
Washington, D.C.   20301

Dr. John E. Walsh
Wilder Laboratory
Department of Physics (HB 6127)
Dartmouth College
Hanover NH   03755

Dr. Jiunn-Ming Wang
Brookhaven National Laboratories
Associated Universities, Inc.
Upton, L.I., NY   11973

Dr. Roger W. Warren
Los Alamos National Scientific Lab.
P.O. Box 1663
Los Alamos, NM   87545

Dr. J. Watson
Los Alamos National Laboratory
P. O. Box 1663
Los Alamos, NM 87545

Dr. Mark Wilson
Natl. Inst. of Standards and Tech.
Bldg. 245, Rm. B-119
Gaithersburg, MD   20899

Dr. J. Wurtele
M.I.T.
NW 16-234
Plasma Fusion Center
Cambridge, MA   02139

Dr. Ming Xie
Dept. of Physics
Stanford University
Stanford, CA   94305

Dr. Simon S. Yu
Lawrence Livermore National Laboratory
P. O. Box 808
Livermore, CA 94550

Naval Research Laboratory
Washington, DC 20375-5000
   Code 2630
   Timothy Calderwood

Records (1 copy)

22